Contents lists available at ScienceDirect

Atmospheric Environment

Impacts of boundary layer mixing on pollutant vertical profiles in the lower troposphere: Implications to satellite remote sensing

Jin-Tai Lin*, Michael B. McElroy

School of Engineering and Applied Sciences, Harvard University, Cambridge, MA 02138, USA

ARTICLE INFO

ABSTRACT

Mixing in the planetary boundary layer (PBL) affects vertical distributions of air tracers in the lower troposphere. An accurate representation of PBL mixing is critical for chemical-transport models (CTMs) for applications sensitive to simulations of the vertical profiles of tracers. The full mixing assumption in the widely used global CTM GEOS-Chem has recently been supplemented with a non-local PBL scheme. This study analyzes the impact of the non-local scheme on model representation of PBL mixing, consequences for simulations of vertical profiles of air tracers and surface air pollution, and implications for model applications to the interpretation of data retrieved from satellite remote sensing. The non-local scheme significantly improves simulations of the vertical distributions for NO_2 and O_3, as evaluated using aircraft measurements in summer 2004. It also reduces model biases over the U.S. by more than 10 ppb for surface ozone concentrations at night and by 2−5 ppb for peak ozone in the afternoon, as evaluated using ground observations. The application to inverse modeling of anthropogenic NO_x emissions for East China using satellite retrievals of NO_2 from OMI and GOME-2 suggests that the full mixing assumption results in 3−14% differences in top−down emission budgets as compared to the non-local scheme. The top−down estimate combining the non-local scheme and the Lin et al. inverse modeling approach suggests a magnitude of 6.6 TgN yr^{-1} for emissions of NO_x over East China in July 2008 and 8.0 TgN yr^{-1} for January 2009, with the magnitude and seasonality in good agreement with bottom−up estimates.

© 2010 Elsevier Ltd. All rights reserved.

1. Introduction

Vertical distributions of air tracers in the lower troposphere are influenced by vertical mixing within the planetary boundary layer (PBL) (Holtslag, 2002; Stull, 2003). Stronger mixing, including a deeper PBL and stronger interactions of tracers from different altitudes in the PBL, leads to more uniform vertical distributions of air tracers in the lower troposphere. On the contrary, weaker PBL mixing tends to result in greater vertical gradients for air tracers. The magnitude of PBL mixing varies significantly in both space and time (Stull, 2003). For example, the depth of the PBL in summer varies by a factor of 2 or more between the eastern and western U.S. in the afternoon and by a factor of 10 or so from night to day (Lin et al., 2008). An accurate representation of PBL mixing is critical for simulation of air tracers in the lower troposphere (Holtslag, 2002).

Mixing in the PBL is driven by turbulence with chaotic characteristics. As a result, the set of dynamic equations specifying the temporal variation of PBL mixing includes more unknowns than the number of equations; thus parameterizations have to be implemented for certain unknowns in order to simulate the evolution of PBL mixing (Stull, 2003). Distinguished primarily by the extent of parameterization, several types of PBL mixing scheme have been employed in global and regional climate and chemistry models (Holtslag and Boville, 1993; Holtslag, 2002; Stull, 2003; http://www.mi.unihamburg.de/Mesoscale-transport-or-chemistry-transportmodel.676.0.html). The first-order 'local' mixing scheme derived based on K-theory (e.g., Louis et al., 1982) assumes that mixing for heat, water vapor and air tracers occurs only between adjacent layers of the PBL, and that the magnitude of mixing is determined by the eddy diffusion coefficient and local gradients of corresponding scalars. In particular, the eddy diffusion coefficient is diagnosed using other meteorological parameters. The local scheme is unable to simulate the PBL-wide mixing by large eddies in the case of an unstable PBL (Holtslag and Boville, 1993; Holtslag, 2002; Stull, 2003). Another type of local mixing scheme relates the eddy diffusion coefficient to the turbulent kinetic energy (TKE) and attempts to solve for the evolution of TKE by equation sets with 1.5 or higher order closure (e.g., Mellor and Yamada, 1982). These schemes are more complicated, and may not necessarily improve the simulation of PBL mixing as a consequence of

---

* Corresponding author. Harvard University, Cruft Lab Room 211A, 19 Oxford St., Cambridge, MA 02138, USA. Tel.: +1 617 496 6365; fax: +1 617 384 8016.
E-mail address: jlin5@seas.harvard.edu (J.-T. Lin).

complex model interactions and uncertainties associated with assumptions concerning the unknowns (Holtslag, 2002). In addition, a number of so-called 'non-local' mixing schemes have been proposed to improve the simulation of mixing when the PBL is unstable (Holtslag, 2002). These schemes typically incorporate a 'non-local' term driving mixing across the PBL, allowing for the effect of large eddies. When the PBL is stable, the non-local term vanishes and the behavior of non-local schemes is similar to that of local mixing schemes (Holtslag and Boville, 1993; Holtslag, 2002). While non-local schemes with higher order closure exist, the most popular non-local schemes employed in global and regional models are based on first-order closure; with relatively simple formulation and computation, they are capable of simulating the PBL mixing under different conditions. One such non-local scheme was presented by Holtslag and Boville (1993) (see detailed discussions in Section 2.1) and is employed widely in many state-of-the-art global and regional models, such as MOZART (Horowitz et al., 2003), TM5 (Krol et al., 2005), CAM3 (Collins et al., 2006) and RegCM3 (Pal et al., 2007). Similar non-local schemes are incorporated in MM5 (Hong and Pan, 1996) and several observation assimilations, including the National Aeronautics and Space Administration (NASA) GOES-5 (Lock et al., 2000) and the European Centre for Medium-Range Weather Forecasts (ECMWF) ERA-40 (Troen and Mahrt, 1986).

GEOS-Chem is a popular and well-known global chemical-transport model (CTM) used by more than 50 research groups worldwide for studies of sources, sinks and transport of gaseous and aerosol tracers in the troposphere; its nested version has been used for studying regional air quality in Asia and North America (http://www.as.harvard.edu/chemistry/trop/geos/). The last model meeting in April 2009 accommodated more than 150 researchers from around the world. And hundreds of peer-reviewed papers associated with the model have been published (e.g., http://www.as.harvard.edu/chemistry/trop/recentpapers.html). Until now, the model incorporates a relatively simple representation of mixing in the PBL. It assumes that tracers are fully mixed within the PBL, i.e., the volume mixing ratio for any given tracer is constant below the PBL top at each simulation time step. Also, effects of surface emissions and dry depositions are distributed uniformly throughout the PBL. As discussed in Section 2.1, this assumption tends to overestimate vertical mixing except under conditions where the PBL is extremely unstable. This deficiency has significant consequences for a range of applications of the model. To improve the simulation of PBL mixing in GEOS-Chem, the non-local mixing scheme formulated by Holtslag and Boville (1993) was implemented recently; and it received enormous interests across the GEOS-Chem community. Using MOZART simulations, Lin et al. (2008) showed that the Holtslag and Boville (1993) scheme reduces biases for surface ozone during nighttime by as much as 15 ppb over the U.S. in summer 1999, as compared to the full-mixing assumption. This paper extends our previous work by analyzing impacts of the improved PBL representation for GEOS-Chem simulations from a variety of aspects, including vertical distributions of gaseous tracers in the lower troposphere, diurnal variation of surface air pollution, and implications for model applications (see below).

Improvements in the representation of PBL mixing in GEOS-Chem have important implications for applications to the interpretation of satellite remote sensing data for tropospheric air pollution. Satellite remote sensing has been used intensively in the analysis of surface and tropospheric gaseous tracers, especially in regions where ground and airborne measurements are scarce (Martin et al., 2003, 2006; Boersma et al., 2004; Jaegle et al., 2005; Zhang et al., 2006; Emmons et al., 2007, 2009; Wang et al., 2007; Boersma et al., 2008b; Martin, 2008; Millet et al., 2008; van der A et al., 2008; Zhang et al., 2008; Lin et al., 2009; Mijling et al., 2009; Zhao and Wang, 2009). Satellite instruments measure ultraviolet, visible or infrared radiation from the top of the atmosphere affected by absorption by specific gaseous tracers. The observed radiance is converted to derive vertical column densities (VCDs) of the tracers (e.g., O_3, NO_2, HCHO, etc.) (Martin et al., 2003, 2006; Boersma et al., 2004; Ziemke et al., 2006; Boersma et al., 2007; Millet et al., 2008) or mixing ratios at particular altitudes (e.g., O_3 and CO) (Zhang et al., 2006; Emmons et al., 2007, 2009). The sensitivity of satellite observed radiation to changes in tracer concentrations depends on altitude as well as on other factors (Boersma et al., 2004, 2007; Zhang et al., 2006). This dependence is represented in terms of the so-called 'averaging kernel'. Retrieved VCDs or mixing ratios provide therefore a proxy for actual VCDs or mixing ratios. To analyze characteristics (sources, sinks, etc.) of tracers, retrieval products are compared with counterparts derived from independent CTM simulations. To minimize the impact of the dependence of satellite sensitivity on altitude, simulated concentrations of tracers at different altitudes are multiplied by the averaging kernel in deriving proxies for simulated VCDs or mixing ratios corresponding to the retrievals (Boersma et al., 2004; Zhang et al., 2006; Lin et al., 2009). This results in a dependence of proxy simulated VCDs or mixing ratios on the vertical shape of tracer concentrations as defined by the model. Since the modeled vertical shape is sensitive to PBL mixing, the newly implemented non-local scheme is expected to enhance the performance of GEOS-Chem in applications to satellite remote sensing. This study analyzes the effect of the two PBL mixing representations on the GEOS-Chem interpretation of satellite NO_2 data used in deriving surface emissions of nitrogen oxides ($NO_x \equiv NO + NO_2$). GEOS-Chem has been employed extensively in such inverse modeling studies (Martin et al., 2003, 2006; Jaegle et al., 2005; Wang et al., 2007; Lin et al., 2009). The impact of PBL mixing is particularly significant for this application, as NO_x is concentrated in the lower troposphere where the influence of PBL mixing is greatest.

Descriptions of GEOS-Chem are presented in Section 2, including a detailed analysis of the two PBL schemes. Section 3 illustrates the impact of the treatment of PBL mixing on the simulation of vertical distributions of air tracers in the lower troposphere, using aircraft measurements over the U.S. and Canada in summer 2004. Section 4 evaluates the impact of the different PBL schemes on the simulation of diurnal variations of surface air pollution over the U.S. The non-local scheme is found to result in simulations significantly improved relative to results derived using the full mixing assumption. Implications of the improved PBL mixing representation for applications to the interpretation of satellite remote sensing data are illustrated in Section 5, where GEOS-Chem and satellite NO_2 data are used to estimate the magnitude of anthropogenic NO_x emissions in China. Concluding remarks are presented in Section 6.

2. Model

GEOS-Chem (v08-01-01; http://www.as.harvard.edu/chemistry/trop/geos/) is driven by the GEOS-5 assimilation of meteorological data from the NASA Global Modeling and Assimilation Office. It is run at a resolution of $2°$ lat by $2.5°$ long with 47 vertical layers, each of the lowest 10 layers having a thickness of ~130 m. All of the simulations in this study were conducted using full HO_x–NO_x–VOC–CO–O_x chemistry.

Anthropogenic emissions of gaseous tracers were taken from the global dataset EDGAR (Olivier and Berdowski, 2001), replaced by regional emission inventories over specific regions. The NEI99 emission dataset is adopted for the U.S., but with emissions for NO_x from power plants and industry reduced by 50% (Hudman et al., 2007) and with emissions for CO from all anthropogenic sources reduced by 60% (Hudman et al., 2008) over the eastern U.S. The INTEX-B emission inventory for 2006 (Zhang et al., 2009) is used for

Asia, distinguishing four major sectors: industry, power plants, transportation, and residential.

Emissions from biomass burning are taken from the GFED2 dataset (van der Werf et al., 2006). Emissions of NO_x from soil are calculated using the scheme introduced by Yienger and Levy (1995). Emissions of NO_x from lightning are evaluated using the scheme presented by Price et al. (1997), adopting the 'C' shape profile proposed by Pickering et al. (1998).

2.1. PBL mixing schemes

Up to now, all versions of GEOS-Chem have assumed full mixing in the PBL. Concentrations, surface emissions, and dry depositions for individual species are assumed to be distributed evenly below the top of the PBL as specified in meteorological datasets (GEOS-5 here). This results in the strongest possible PBL mixing under all possible meteorological conditions. The assumption is reasonable when the actual PBL is extremely unstable, e.g., for a hot summer afternoon over the U.S. Midwest under cloud free conditions. It will seriously overestimate, however, vertical mixing when the PBL is modestly or weakly unstable, neutral, or stable, e.g., for a cool summer night with clear sky and weak winds.

The non-local scheme evaluates the extent of vertical mixing within the PBL taking into account the magnitude of the instability. The detailed formulation and description of the scheme were presented by Holtslag and Boville (1993) and Lin et al. (2008). In the absence of a net flux of sensible and latent heat from the Earth surface to the atmosphere, mixing in the PBL is determined by the first-order local mixing scheme. In the presence of a net flux of heat from the Earth surface to the atmosphere, the model PBL is statically unstable, with the magnitude of the instability determined by the magnitude of net heat flux as well as by the vertical gradient of virtual potential temperature. In this case, in addition to the 'local' mixing between adjacent layers, the non-local scheme introduces a 'non-local' term to drive mixing of tracers in the PBL, allowing thus for the effect of large eddies. The magnitude of such PBL-wide mixing depends on the magnitude of the instability. For the case of an extremely unstable PBL, the non-local scheme yields results similar to those obtained using the full mixing assumption. Overall, the non-local scheme allows for a more realistic simulation of vertical mixing within the PBL, particularly when the PBL is either neutral or stable.

3. Vertical profiles in the lower troposphere

Measurements from the DC-8 aircraft during the NASA INTEX-NA campaign (Singh et al., 2006) and from the WP-3D aircraft during the National Oceanic and Atmospheric Administration (NOAA) ICARTT campaign (Fehsenfeld et al., 2006) in July–Mid August 2004 provide valuable information on vertical distributions
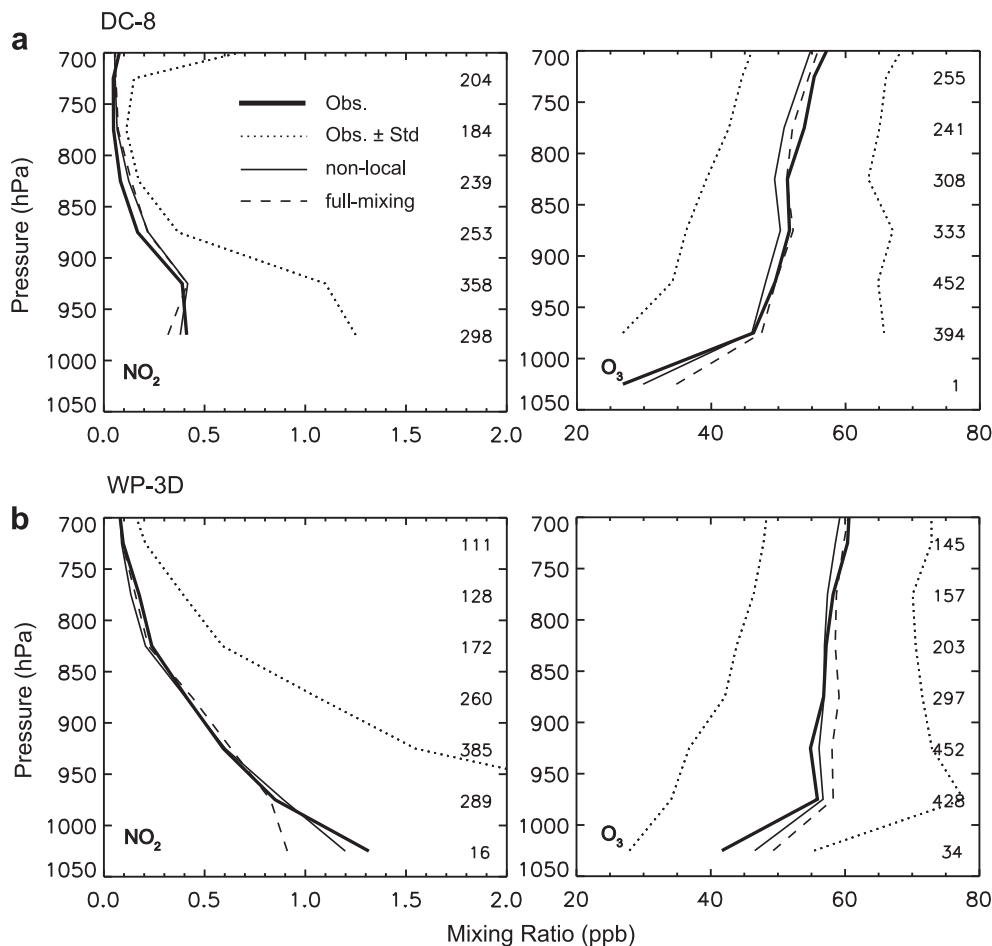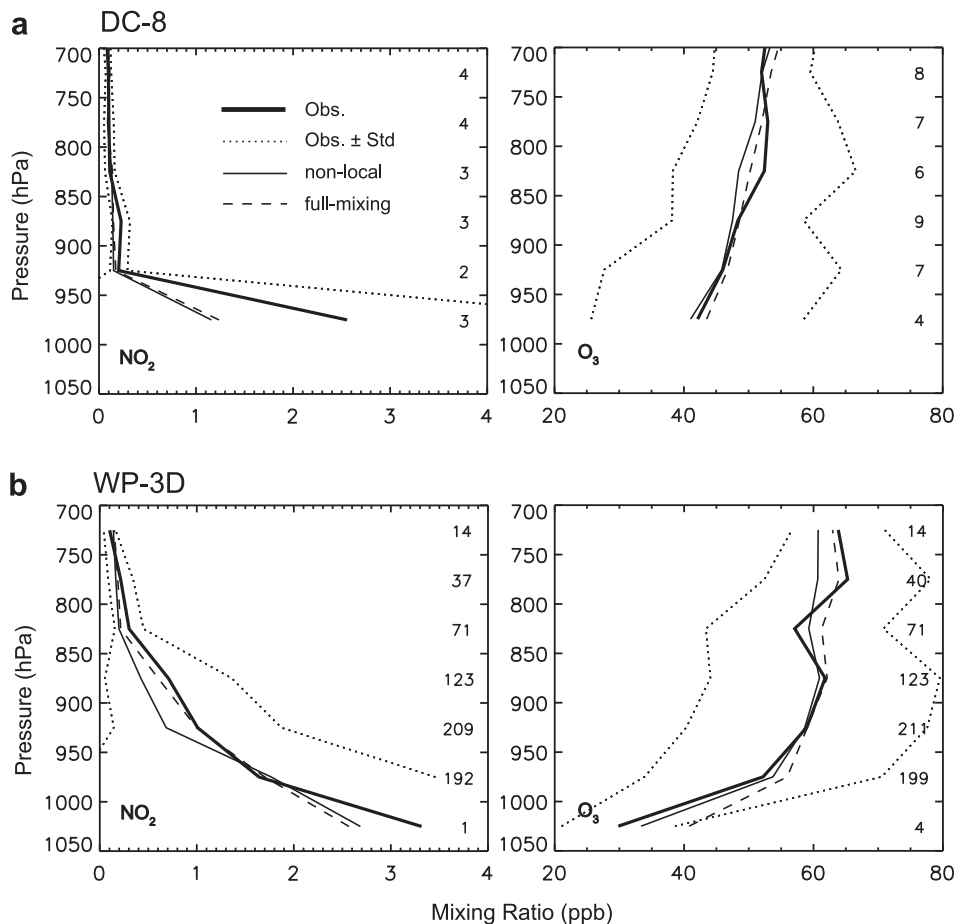

Fig. 1. Daytime (8:00am–8:00pm) comparisons between simulated NO_2 and O_3 vertical profiles and aircraft measurements from (a) DC-8 during the NASA INTEX-NA campaign and (b) WP-3D during the NOAA ICARTT campaign in summer 2004. Thick solid lines depict aircraft measurements, thin solid lines depict simulations driven by the non-local PBL scheme, and thin dashed lines depict simulations with full mixing assumption. The numbers of 1-min measurements for each vertical bin (sized at 50 hPa) are shown on the right of each panel. Simulated NO_2 and O_3 mixing ratios are sampled along the flight tracks. Simulated NO_2 mixing ratios shown in (b) have been scaled by 140%.

of various tracers in the lower troposphere. The DC-8 flights covered a large portion of the U.S. and southern Canada, measuring tracers at a height of several hundred meters or more above the ground. The WP-3D flights focused significantly on the Northeast U.S. with particular attention to studying the vertical distributions of tracers in the PBL. Detailed flight track information was presented by Hudman et al. (2007). In this section, 1-min average data for NO_2 and O_3 from DC-8 and WP-3D were used to evaluate the impact of different representations of PBL mixing in GEOS-Chem on the simulation of vertical profiles for key tracers in the lower troposphere (Figs. 1 and 2). NO_2 was measured by Laser Induced Florescence on the DC-8 (Bertram et al., 2007) and by photolysis-chemiluminescence on the WP-3D (Ryerson et al., 1999); while O_3 was measured by NO/O_3 chemiluminescence on both aircrafts (Ryerson et al., 1998; Avery et al., 2001). Concentrations of the different tracers were evaluated along the flight tracks using the model to ensure consistent comparison with measurements.

Several criteria were used to select measurement data for appropriate model evaluation. Since we focus on vertical profiles, we chose to emphasize measurements taken when the aircrafts were either descending or ascending. Specifically, for a given measurement, if the maximum and minimum altitudes of the aircraft within 2.5 min (both forward and backward) differ by less than 50 m, the corresponding measurements were excluded from the analysis. In addition, measurements with an O_3/CO concentration ratio of 1.25 or larger were excluded to eliminate the influence of stratospheric air intrusions (Hudman et al., 2007). And measurements with HCN mixing ratios larger than 500 ppt or CH3CN mixing ratios larger than 225 ppt were also excluded in order to eliminate the influence of fresh wildfire plumes (Hudman et al., 2007).

To enhance comparisons with the WP-3D data for NO_2, a special adjustment was imposed on profiles simulated with both PBL schemes. The present study uses anthropogenic emissions of NO_x estimated by Hudman et al. (2007) for the U.S., which are much lower than the NEI99 emissions. For the Northeast U.S., the lower emissions are inconsistent with findings of Martin et al. (2006) who suggested that the NEI99 dataset underestimated NO_x emissions for this region. Hudman et al. (2007) concluded that large uncertainties are associated with NO_x emissions for the Northeast U.S. Using the reduced emissions proposed by Hudman et al. (2007), NO_2 concentrations simulated here are much lower than the WP-3D measurements at all altitudes in the lower troposphere. Nonetheless, the magnitude of surface emissions is expected to have a relatively minor impact on the shape of the vertical profile for NO_2 over the Northeast U.S., which is determined mainly by PBL mixing. Thus we scaled the simulated NO_2 concentrations by an arbitrary 140% to match the observed NO_2 burden below 700 hPa from WP-3D; no such adjustment was applied for purposes of comparison with the DC-8 data. A sensitivity simulation using the non-local scheme, in which anthropogenic and soil emissions of NO_x were scaled by 140% over the region of 83.75°W−58.75°W and 37°N−51°N, resulted in a vertical distribution of NO_2 below 700 hPa

Fig. 2. Nighttime (8:00pm−8:00am) comparisons between simulated NO_2 and O_3 vertical profiles and aircraft measurements from (a) DC-8 during the NASA INTEX-NA campaign and (b) WP-3D during the NOAA ICARTT campaign in summer 2004. Thick solid lines depict aircraft measurements, thin solid lines depict simulations driven by the non-local PBL scheme, and thin dashed lines depict simulations with full mixing assumption. The numbers of 1-min measurements for each vertical bin (sized at 50 hPa) are shown on the right of each panel. Simulated NO_2 and O_3 mixing ratios are sampled along the flight tracks. Simulated NO_2 mixing ratios shown in (b) have been scaled by 140%.

that is essentially the same as the corresponding simulation based on the arbitrary 140% scaling assumption (Fig. 3). This indicates that the shape of the vertical profile of NO_x in the lower troposphere over the Northeast U.S. is relatively independent of the magnitude of surface emissions, and that scaling NO_2 concentrations by 140% represents an appropriate adjustment for the purpose of evaluating the PBL schemes.

Figs. 1 and 2 compare observed and modeled vertical distributions below 700 hPa for NO_2 and O_3. Simulated NO_2 profiles are scaled by 140% for comparison with WP-3D measurements. Tracer concentrations at different heights were averaged into several vertical intervals with a depth of 50 hPa in each interval. Comparisons were selected to separately reflect daytime (8:00am–8:00pm local time; Fig. 1) and nighttime (8:00pm–8:00am; Fig. 2) conditions in order to differentiate vertical profiles of tracers under different states of the PBL.

3.1. Daytime (8:00am–8:00pm)

During the daytime (Fig. 1), the observed profile for NO_2 indicates a rapid reduction in concentration with increasing height, from 0.4 ppb at 975 hPa to 0.1 ppb at 800 hPa for DC8 measurements and from 1.3 ppb below 1000 hPa to 0.2 ppb at 800 hPa for WP-3D. This is due to the short lifetime of NO_2 combined with the fact that NO_x in the lower troposphere is derived primarily from emissions at the surface. The simulation driven by the non-local scheme compares well with the observed data, with a comparatively small bias below 900 hPa. From 900 hPa to 700 hPa, the modeled NO_2 concentrations exceed the DC8 values while being slightly lower than the WP-3D measurements. By comparison, the simulation assuming full PBL mixing yields lower NO_2 concentrations near the surface as compared with either measurement set. Comparisons with WP-3D measurements clearly indicate that the full mixing assumption underestimates the vertical gradient of NO_2 in the lower troposphere.
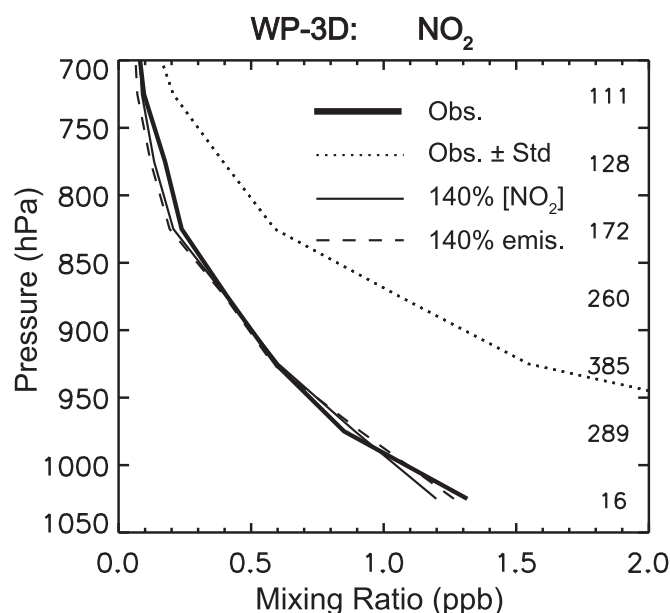

Fig. 3. Comparisons of NO_2 vertical profiles during the daytime (8:00am–8:00pm) between the simulation with resulted NO_2 mixing ratio arbitrarily scaled by 140% (thin solid line) and the sensitivity simulation with anthropogenic and soil emissions of NO_x scaled by 140% (thin dashed line). The non-local mixing scheme is used in both simulations, and modeled NO_2 mixing ratios are sampled along the flight tracks of WP-3D. Also presented are measurements from WP-3D (thick solid line). The numbers of 1-min measurements for each vertical bin (sized at 50 hPa) are shown on the right.

Observed profiles for O_3 indicate a gradual increase of concentration with height (Fig. 1). This feature is caused mainly by the vertical gradient of O_3 in the morning; in the afternoon, O_3 is relatively well mixed in the PBL (see also Lin et al., 2008). The non-local scheme results in concentrations 3–5 ppb higher than measurements from both aircrafts below 1000 hPa. Above 1000 hPa, model concentrations of O_3 are up to 4 ppb lower than values observed from the DC8, while close to measurements by the WP-3D. By comparison, the simulation assuming full mixing in the PBL results in concentrations of O_3 1–5 ppb larger than values obtained using the non-local scheme. This is because the non-local scheme results in less efficient and more realistic production of ozone (Lin et al., 2008).

The underestimate of O_3 above 1000 hPa using the non-local scheme relative to the DC8 measurements is attributed primarily to an underestimate of wildfire emissions in Alaska and Canada that impacted background ozone concentrations during the period of aircraft measurements. The best estimate for wildfire emissions of CO in summer 2004 is approximately 30 Tg (Turquety et al., 2007), approximately twice the magnitude implied by the GFED2 dataset adopted here. In a sensitivity simulation, emissions from biomass burning were doubled, resulting in little underestimate of O_3 at most altitudes relative to the DC-8 measurements (Fig. 4). Meanwhile, the ozone bias was decreased (increased) above (below) 800 hPa by 0–2 ppb as compared to the WP-3D measurements (Fig. 4). It is expected that if biomass burning emissions were doubled, the full mixing assumption would lead to an overestimate of O_3 concentrations in the lower troposphere as compared to both measurement datasets. The sensitivity simulation indicates also that the underestimate of wildfire emissions has little influence on profiles derived for NO_2, a consequence of the short lifetime of NO_x.

The likely underestimate of NO_x emissions over the Northeast U.S. affects also the simulations of O_3. As shown in Fig. 5, the sensitivity simulation with NO_x emissions scaled by 140% resulted in a 2–5 ppb increase in O_3 concentrations in the lower troposphere over the Northeast U.S., an increase of ~2 ppb near the surface. Nonetheless, the non-local scheme persists in producing a bias smaller than that derived using the full mixing assumption.

3.2. Nighttime (8:00pm–8:00am)

The DC-8 measurements were taken mainly during daytime. The number of nighttime measurements is consequently insufficient to allow definite conclusions to be drawn as to the relative merits of the two PBL schemes (Fig. 2a). The WP-3D measurements indicate a much larger vertical gradient at night as compared to day for both tracers (Fig. 2b). The observed NO_2 mixing ratio decreases from ~3.3 ppb below 1000 hPa to 0.3 ppb at 800 hPa, while O_3 increases from 30 ppb below 1000 hPa to more than 60 ppb at 800 hPa. Vertical gradients of NO_2 calculated using both PBL schemes are weaker than the observation. Simulated results for O_3 are in much better agreement with the WP-3D measurements below 800 hPa when the non-local scheme is used, with the bias near the surface ~7 ppb smaller than the simulation assuming full PBL mixing.

3.3. Summary

Overall, the non-local scheme is found to improve GEOS-Chem simulations of the vertical distributions of NO_2 and O_3 in the lower troposphere, as indicated by comparisons with aircraft measurements from the DC-8 and WP-3D. The improvement in NO_2 simulations is most significant during daytime, especially in terms of the shape of the vertical profile. The enhancement for O_3 persists throughout the day, especially near the surface. These improvements impact not only simulations of surface air pollution, but have important implications also for applications of the model to
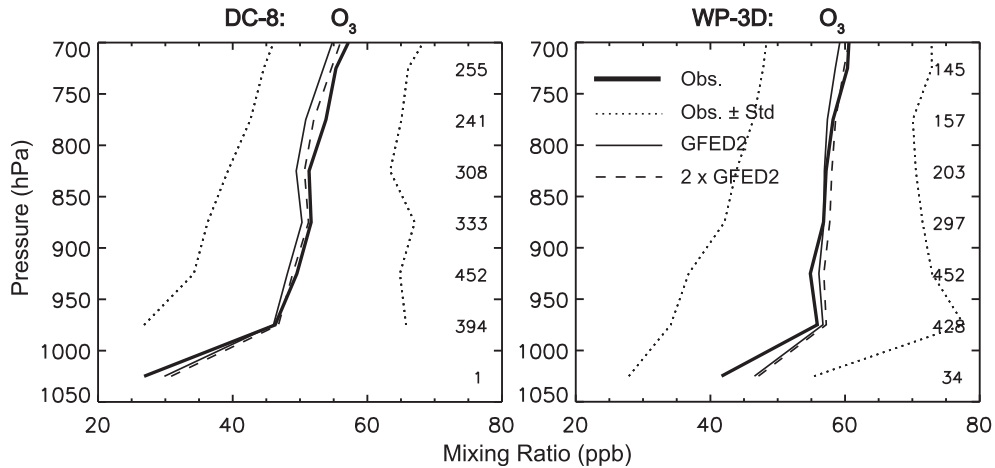
Fig. 4. Comparisons of O₃ vertical profiles during the daytime (8:00am–8:00pm) between the simulation with GFED2 biomass burning emissions (thin solid lines) and the sensitivity simulation with 2 times GFED2 biomass burning emissions (thin dashed lines). The non-local mixing scheme is used in both simulations, and modeled O₃ mixing ratios are sampled along the flight tracks. Also presented are the aircraft measurements (thick solid lines). The numbers of 1-min measurements for each vertical bin (sized at 50 hPa) are shown on the right of each panel.

analysis of satellite remote sensing data. In particular, the improved vertical shape of daytime NO₂ concentrations has important consequences for inverse modeling of NOₓ emissions using satellite NO₂ retrievals, as discussed in Section 5.

4. Diurnal variation of surface air pollution

Vertical mixing in the PBL has important influences on the magnitude and temporal variability of surface air pollution. This section analyzes differences in GEOS-Chem simulations of the diurnal variation of surface O₃ obtained using the different PBL schemes for July 2004 over four U.S. regions: Northeast, Midwest, Southeast, and Southwest. Rural site measurements from the U.S. Environmental Protection Agency (EPA) Air Quality System (AQS) are used for model evaluations. Following Lin et al. (2008), observed O₃ concentrations at all sites within the boundaries of a given model gridcell were averaged to represent measurements for the gridcell; and gridcells with available observations were averaged in calculating regional mean O₃ concentrations.

As shown in Fig. 6, O₃ concentrations exhibit a maximum during the afternoon resulting primarily from fast photochemical production driven by strong solar radiation, high temperature, and large anthropogenic and natural emissions of precursors. They exhibit a minimum around sunrise reflecting titration by NOₓ and the influence of dry deposition during the night. Weak nighttime PBL mixing inhibits transport to the surface of air plumes with high O₃ content from higher altitudes. The non-local scheme predicts weaker and more realistic mixing at night as compared with the full-mixing assumption, resulting in lower concentrations of ozone near the surface. As a consequence, the positive bias of the model at night is reduced by up to more than 10 ppb over the four regions. During the afternoon, both schemes simulate strong mixing in the PBL; results for O₃ are consequently similar. Nonetheless, the non-local scheme is found to produce more realistic results as compared with the full-mixing assumption, with 2–5 ppb less bias over the Midwest, Northeast and Southeast. Simulations with both schemes over the Southwest underestimate observed O₃ concentrations in the afternoon. The dependence of model results on the different PBL schemes found here is similar to that presented by Lin et al. (2008) using MOZART.

The overall performance of GEOS-Chem for simulation of surface ozone is similar to that of MOZART (Lin et al., 2008). Depending on
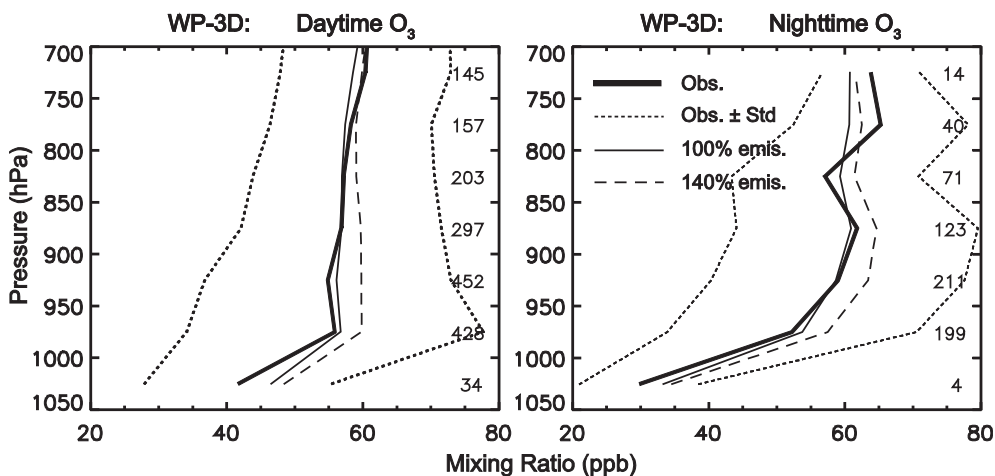
Fig. 5. Comparisons of O₃ vertical profiles between the simulation with NOₓ emissions un-scaled (thin solid line) and the sensitivity simulation with anthropogenic and soil emissions of NOₓ scaled by 140% (thin dashed line). The non-local mixing scheme is used in both simulations, and modeled O₃ mixing ratios are sampled along the flight tracks of WP-3D. Also presented are measurements from WP-3D (thick solid line). The numbers of 1-min measurements for each vertical bin (sized at 50 hPa) are shown on the right of each panel.
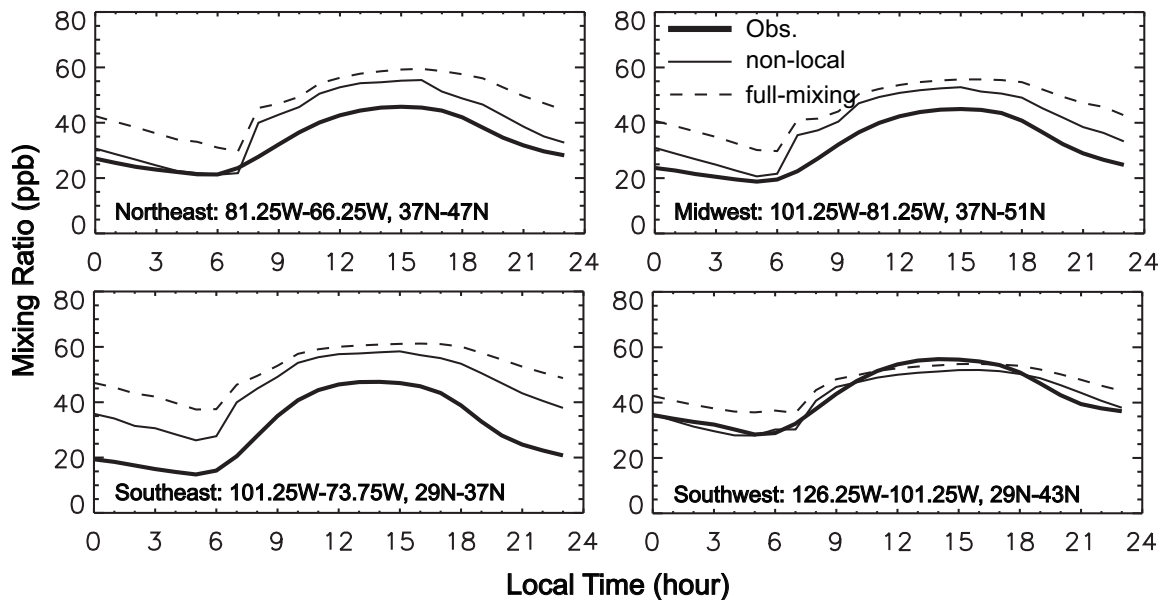
Fig. 6. Observed and simulated monthly mean diurnal variations of surface ozone concentrations over various regions of the U.S. in July 2004. Thick solid lines depict rural site measurements from the U.S. EPA AQS, thin solid lines depict simulations driven by the non-local PBL scheme, and thin dashed lines depict simulations with full mixing assumption. Boundary specifications of the regions are visualized in Fig. 7a.

the choice of PBL scheme, the model overestimates peak ozone concentrations in the afternoon by 10–15 ppb over the eastern U.S. (Fig. 6). Biases are found also in the spatial distributions of maximum daily 8-h average ozone concentrations (Fig. 7a). These may be related to an overestimate of mixing of NO_x and volatile organic compounds (VOCs) (isoprene in particular), due to the coarse spatial resolution of the model, resulting thus in an enhanced efficiency for ozone production (Wild and Prather, 2006; Lin et al., 2008). Also, it is likely that dry deposition of ozone in summer over the eastern U.S. is underestimated by at least 30% on the basis of the Wesely (1989) scheme used in GEOS-Chem (Wesely and Hicks, 2000; Lin et al., 2008) Lin et al. (2008) found that a 30% increase in ozone dry deposition reduces ozone biases by 2–6 ppb over the eastern U.S. Furthermore, nighttime concentrations of ozone are overestimated in GEOS-Chem by 15–20 ppb over the Southeast, even with use of the non-local scheme (Fig. 6). This overestimate can be attributed partially to the large biases along the south and southeast coasts where the coarse resolution of the model is insufficient to capture the land-ocean contrast (Fig. 7b). Similar biases are found in simulations using MOZART (Lin et al., 2008).

5. Implications for inverse modeling of NO_x emissions using satellite NO_2 retrievals

This section evaluates impacts of PBL mixing representations in GEOS-Chem on results derived for inverse modeling of anthropogenic NO_x emissions based on satellite retrievals of tropospheric NO_2 VCDs. GEOS-Chem simulations driven by the full mixing assumption have been used widely in such inverse modeling studies (Martin et al., 2003, 2006; Jaegle et al., 2005; Wang et al., 2007). Lin et al. (2009) presented the first application of the model using the non-local scheme. Two satellite level-2 NO_2 VCD datasets from the Royal Netherlands Meteorological Institute (KNMI) were used in this analysis, including GOME-2 (version TM4NO2A v1.10) (Boersma et al., 2004) and OMI (version DOMINO v1.0.2) (Boersma et al., 2007). GOME-2 is onboard the satellite MetOp-A with an overpass time of ~9:30am local time, with OMI on AURA with an overpass time of ~1:30pm. Similar retrieval

methods were used to derive the two NO_2 products (Boersma et al., 2004, 2007; Lin et al., 2009). Here the level-2 data were gridded onto $2°$ lat $× 2.5°$ long to facilitate comparison with GEOS-Chem simulations. Details of the retrievals are given by Lin et al. (2009).

Top–down emissions from anthropogenic sources in East China are derived here for July 2008 and January 2009; they are used to evaluate the influence of the different PBL mixing representations on results from such inverse modeling studies, including impacts on conclusions drawn concerning the seasonality of emissions. OMI data are available since October 2004; GOME-2 data since April 2007. We focus on East China ($103.75°E$–$123.75°E$, $19°N$–$45°N$), where anthropogenic emissions of NO_x are large and have increased rapidly in recent years. Also, individual contributions of anthropogenic emissions in this region, including their diurnal variations, are readily available and can be incorporated in the inverse modeling approach described by Lin et al. (2009) (see Section 5.1).

Spatial distributions of annual mean anthropogenic emissions of NO_x from all sectors over East China as defined in the a priori dataset from the INTEX-B mission are presented in Fig. 8a; the seasonal variation of anthropogenic emissions is not resolved in this dataset. Emissions are found to be large over industrial and urban centers, including Northern East China, the Yangtze River Delta, and the Pearl River Delta, lower over rural areas. The emissions are ~5.7 TgN yr^{-1} for East China, representing approximately 86% of total Chinese anthropogenic emissions. The best estimate of diurnal profiles for individual emission sources (Lin et al., 2009) assumed for INTEX-B emissions is presented in Fig. 8b.

5.1. Inverse modeling approaches

Two inverse modeling approaches are examined. The first was proposed by Martin et al. (2003). It derives top–down emissions corresponding to NO_2 retrievals by multiplying daily mean emissions in the a priori dataset by an amount equal to the ratio of retrieved to modeled tropospheric NO_2 VCDs at the overpass time for the satellite (see Eq. (3) in Martin et al. (2003)). In this approach, NO_2 retrievals from a single satellite instrument are used for each derivation. Also, diurnal variations of anthropogenic NO_x emissions
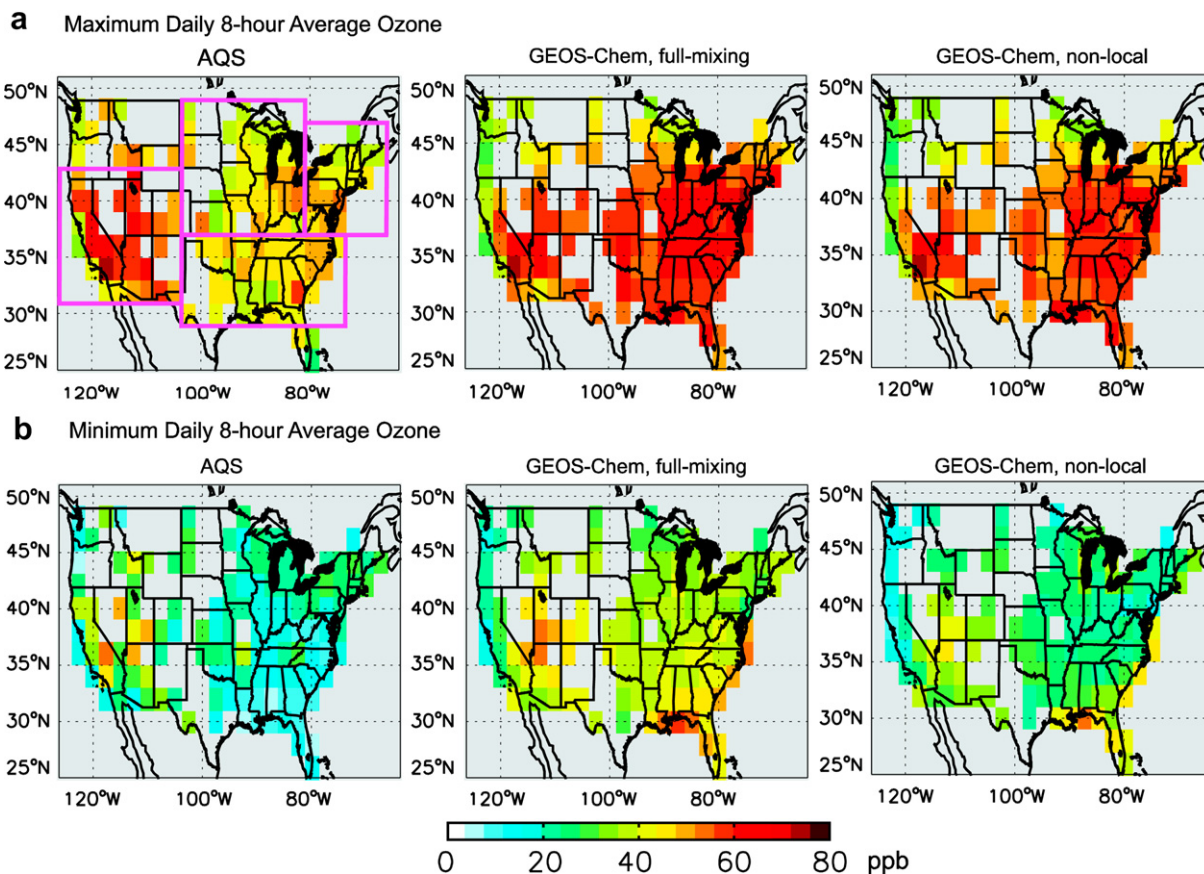
Fig. 7. Observed and simulated monthly mean (a) maximum and (b) minimum daily 8-h average ozone concentrations over the U.S. in July 2004. Gridcells with no observations are shown in gray. The dark pink boxes in (a) (left panel) specify the lateral boundaries of the regions used in Fig. 6. (For interpretation of the references to colour in this figure legend, the reader is referred to the web version of this article.)

are determined by the prescribed temporal profiles used in CTMs. Lin et al. (2009) found that the prescribed profiles may not represent the best understanding of temporal variations of NO_x emissions for many regions, including China. An alternate approach was proposed incorporating multiple satellite NO_2 instruments observing the atmosphere at different times of day, using differences in retrieved NO_2 VCDs between the instruments to estimate NO_x emissions. Top−down emissions from individual anthropogenic sources are derived simultaneously. The formulation of this approach accounts explicitly for diurnal variations of NO_x emissions and concentrations (see Eqs. (7)−(9) in Lin et al. (2009)). In particular, since diurnal profiles of NO_x emissions are defined explicitly in the formulation, they are independent of the profiles prescribed in CTMs. In this study, the same profiles (Fig. 8b) are used both for GEOS-Chem simulations and in the top−down formulation. Detailed derivations and comparisons of the two approaches are given by Martin et al. (2003) and Lin et al. (2009).

The Lin et al. approach can be improved further as follows. For a given model gridcell, the approach derives top−down emissions based on the weighted difference in retrieved NO_2 VCDs between OMI and GOME-2, i.e., OMI − K × GOME-2, where K is a weighting factor equal to the residual fraction of the VCDs observed by GOME-2 at the overpass time of OMI after all loss processes during the time period (see Eq. (6) in Lin et al. (2009)). If this weighted difference is larger (smaller) than its counterpart derived from GEOS-Chem simulations, top−down total emissions will be larger (smaller) than a priori values. Thus the magnitude of top−down emissions is non-linearly related to either retrieval product. In other words, retrieved

VCDs higher than model values might be expected to lead to lower values for top−down as compared to a priori emissions; while retrievals lower than modeled VCDs might lead to top−down emissions larger than a priori values. In estimating emissions from anthropogenic sources, it is expected that the actual anthropogenic emissions will be most likely larger than a priori values if retrieved VCDs from GOME-2 and OMI are both larger than 120% of corresponding model results. Consequently, the final top−down anthropogenic emissions are set as the largest of the a priori and the top−down estimate using the original Lin et al. approach. Concurrently, the final top−down anthropogenic emissions are set not to exceed the a priori values if VCDs modeled at both times of day are greater than 120% of corresponding retrievals.

Satellite retrievals cannot be used alone to differentiate contributions from individual emission sources. To derive top−down emissions of NO_x from anthropogenic sources, assumptions are made on natural emissions in East China. In the top−down dataset, lightning emissions are assumed to be the same as those used in GEOS-Chem, ∼0.37 TgN yr^{-1} in July 2008 and negligible for January 2009. Emissions from soil are taken to be twice as large as emissions adopted in GEOS-Chem based on previous studies (Wang et al., 2004, 2007; Jaegle et al., 2005; McElroy and Wang, 2005; Zhao and Wang, 2009). As such, soil emissions for July 2008 are ∼0.56 TgN yr^{-1} in the a priori dataset as compared to 1.12 TgN yr^{-1} in the top−down result; they are insignificant in January 2009. Emissions from aircraft and biomass burning are assumed to be the same as those used in GEOS-Chem, and their contributions are negligible over East China. The same assumptions were made by Lin et al. (2009).
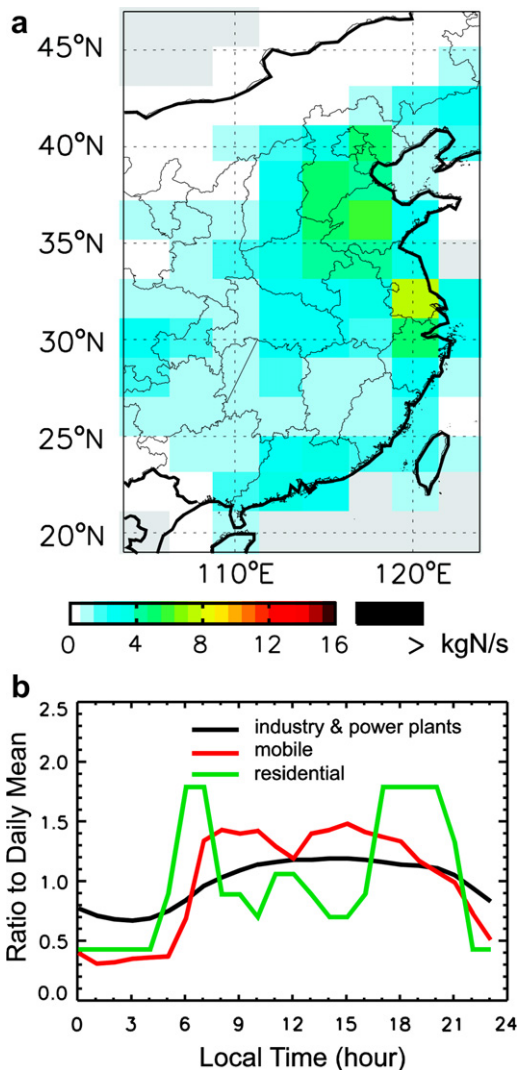
Fig. 8. Spatial distributions of annual mean total anthropogenic emissions of NO_x in East China from the INTEX-B dataset (a) and corresponding diurnal profiles for individual emission sectors (b). These diurnal profiles are used for both GEOS-Chem simulations and the formulation of the Lin et al. inversing modeling approach. In (a), gridcells not covering Chinese lands or with no emissions are shown in gray.

5.2. Top−down anthropogenic emissions

Table 1 compares top−down estimates of anthropogenic emissions for NO_x in East China with bottom−up estimates. For July 2008, top−down anthropogenic emissions calculated by the Martin et al. method are about 7.5 TgN yr^{-1} using the OMI retrievals for inverse modeling and 9.5 TgN yr^{-1} for GOME-2 if GEOS-Chem is driven by the non-local PBL scheme. Assuming full PBL mixing in GEOS-Chem, the Martin et al. method results in a NO_x emission budget of 7.7 TgN yr^{-1} relative to OMI and 8.8 TgN yr^{-1} relative to GOME-2, 3% larger and 7% lower, respectively, than results obtained using the non-local PBL scheme. Using the Lin et al. approach, the full mixing assumption implies emissions of 7.4 TgN yr^{-1} for East China, about 12% larger than values obtained using the non-local scheme.

For January 2009 (Table 1), the non-local scheme results in a budget of 11.3 TgN yr^{-1} for OMI, 14.8 TgN yr^{-1} for GOME-2, over East China, as estimated using the Martin et al. method. Using the Lin et al. approach, top−down emissions are estimated at 8.0 TgN yr^{-1}. Compared to the non-local scheme, the full mixing assumption leads to a budget from OMI (GOME-2) using the Martin et al. method that is 12% (14%) lower; emissions derived are 8% lower when the Lin et al. method is used.

The a priori emissions from the INTEX-B dataset suggest emissions of 5.7 TgN yr^{-1} for East China in 2006, with no seasonality. Assuming that Chinese anthropogenic emissions increased from 2006 to 2008 at a rate of 8% per year as projected from the trend in earlier years (Zhao and Wang, 2009), the bottom−up emissions for 2008 estimated using the INTEX-B dataset would be ~6.7 TgN yr^{-1}, about 17% larger than the a priori. Due to emission control measures targeting the 2008 Beijing Olympics and the 11th Five Year Plan, which have been enforced more strictly since 2007 (http://www.mep.gov.cn/info/gw/gg/200703/t20070302_101268.htm; http://news.xinhuanet.com/newscenter/2009-04/22/content_11233585.htm), the actual emissions for 2008 may be lower than 6.7 TgN yr^{-1} (Lin et al., 2009). Our best estimate for emissions in 2008 derived from the bottom−up dataset is ~6.2 TgN yr^{-1}, 8% larger than the a priori. Additionally, previous bottom−up estimates suggested that anthropogenic emissions of NO_x were ~5% lower in July as compared with the annual mean and ~10% higher in January; the seasonality is due primarily to sources related to domestic heating (Streets et al., 2003; Zhang et al., 2009). Consequently, our bottom−up estimates for NO_x emissions for July 2008 and January 2009 are 5.9 TgN yr^{-1} and 6.8 TgN yr^{-1}, respectively (Table 1). Overall, the Martin et al. method results in emission estimates 31−160% higher than the a priori values, depending on season and on the PBL mixing representations adopted in GEOS-Chem; whereas the Lin et al. method leads to emissions 15−40% larger than the a priori values (Table 1). The top−down estimate incorporating the Lin et al. approach and the non-local scheme, i.e., 6.6 TgN yr^{-1} for July 2008 and 8.0 TgN yr^{-1} for January 2009, is in good agreement with the bottom−up estimate.

The choice of PBL mixing representation in GEOS-Chem can have a significant impact also on inferences concerning the seasonality of emissions (Table 1). Incorporating the non-local scheme, the emission budget for East China in January 2009 estimated using the Martin et al. method is 52% (57%) larger than that for July 2008 based on OMI (GOME-2) retrievals; based on the Lin et al. method, the budget in January 2009 is 22% greater than that for July 2008. Assuming full PBL mixing in GEOS-Chem, the top−down emissions

Table 1
Bottom−up and top−down estimates of anthropogenic emission budgets for NO_x in East China.

	Bottom−up[a]	Top−down					
		Full mixing in the PBL			Non-local mixing		
		OMI (M[b])	GOME-2 (M)	GOME-2 + OMI (L)	OMI (M)	GOME-2 (M)	GOME-2 + OMI (L)
July 2008 (TgN yr^{-1})	5.9	7.7	8.8	7.4	7.5	9.5	6.6
January 2009 (TgN yr^{-1})	6.8	9.9	12.8	7.3	11.3	14.8	8.0
January−July ratio	116%	129%	146%	99%	152%	157%	122%

[a] The bottom−up estimates are derived by increasing the annual mean emissions by 8% from the budget in the INTEX-B dataset, on top of which a seasonal variation is superimposed such that emissions in July and January are 5% lower and 10% higher than the annual mean, respectively.
[b] The letter 'M' denotes the inverse modeling approach proposed by Martin et al. (2003), and 'L' by Lin et al. (2009).

for January 2009 are 29% (46%) larger than for July 2008 based on OMI (GOME-2), as determined using the Martin et al. method; emissions in January 2009 are ∼1% lower than for July 2008 using the Lin et al. inverse modeling approach. The non-local scheme, together with the Lin et al. approach, results in a January-to-July ratio of ∼122% for anthropogenic NO$_x$ emissions, comparable to bottom−up estimates of ∼116% (Streets et al., 2003; Zhang et al., 2009).

Spatially, the general patterns of top−down emissions are similar to those specified in the a priori dataset, independent of PBL schemes and inverse modeling approaches (Figs. 9 and 10). The non-local scheme together with the Martin et al. method leads to higher top−down emissions than the a priori over most regions in both months. Correspondingly, top−down emissions derived using the Lin et al. method are closer to a priori values, especially for July 2008. Differences in top−down results between the two PBL schemes are consistent over most regions. For July 2008, the full mixing assumption using the Martin et al. method leads to higher (lower) emissions relative to the OMI (GOME-2) retrieval than results obtained using the non-local scheme, with larger emissions estimated on the basis of the Lin et al. method (Fig. 9). For January 2009, it results in lower emissions than estimates associated with the non-local scheme, irrespective of inverse modeling approaches (Fig. 10).
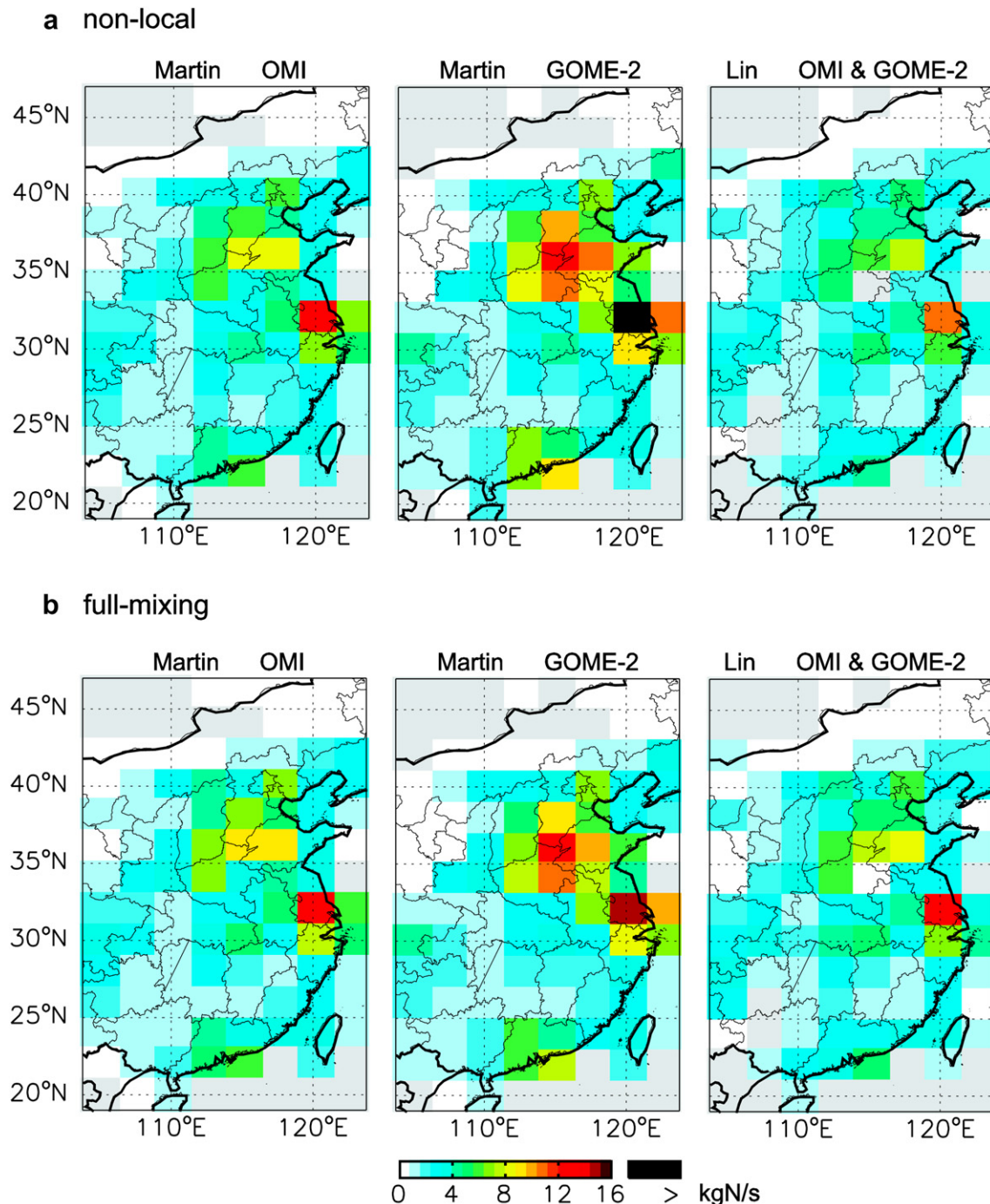
Fig. 9. Top−down estimates of NO$_x$ emissions for July 2008 derived using Martin et al. and Lin et al. approaches. Emission distributions relative to GEOS-Chem simulations driven by the non-local scheme and the full mixing assumption are presented in (a) and (b), respectively. Gridcells not covering Chinese lands or with no emissions are shown in gray.
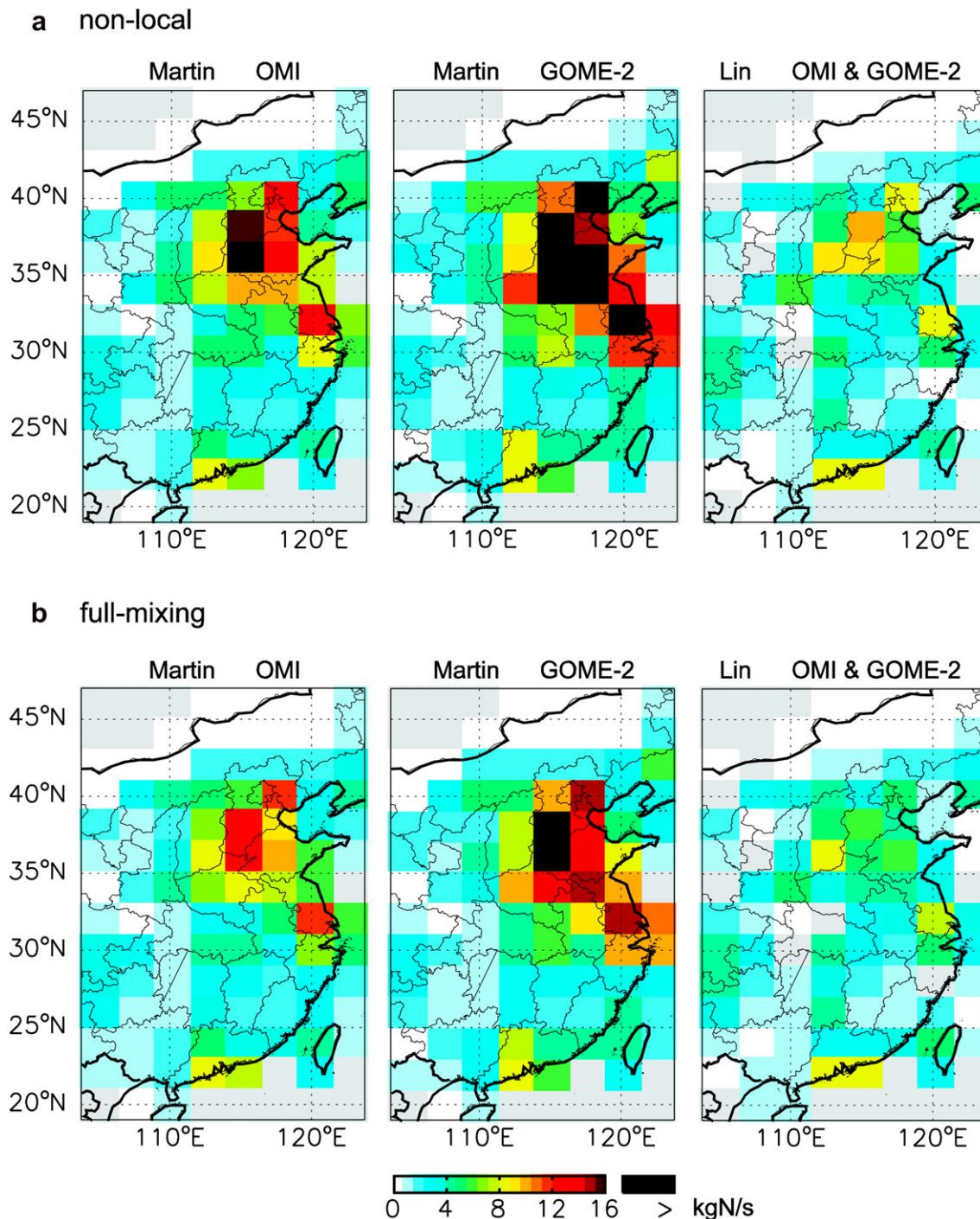
Fig. 10. Top–down estimates of NO$_x$ emissions for January 2009 derived using Martin et al. and Lin et al. approaches. Emission distributions relative to GEOS-Chem simulations driven by the non-local scheme and the full mixing assumption are presented in (a) and (b), respectively. Gridcells not covering Chinese lands or with no emissions are shown in gray.

5.3. Discussion

Both inverse modeling approaches assume that horizontal transport of NO$_x$ has an insignificant impact on top–down estimates for individual model gridcells at a resolution of 2° × 2.5°. The assumption is appropriate for summer when the lifetime of NO$_x$ is only 3–5 h over East China such that only a small fraction of NO$_x$ is transported horizontally between adjacent gridcells (Martin et al., 2003, 2006; Lin et al., 2009). In winter, however, the lifetime of NO$_x$ is longer and horizontal transport between adjacent gridcells

may be expected to have an impact on concentrations in individual gridcells and to complicate consequently top–down estimates for emissions (Boersma et al., 2008a). As a result, spatial distributions of top–down emissions for NO$_x$ over East China may be affected by the neglect of horizontal transport (see more discussions in Lin et al., 2009). Nonetheless, estimates for top–down emission budgets in East China are not impacted significantly. In a sensitivity test, top–down emission budgets were derived by applying each approach to East China as a whole. As such, effects of horizontal transport are minimized since transport among gridcells within the

region does not affect top–down estimates. The resulting emission budgets are within 10% of the corresponding budgets summed over top–down emissions estimated for individual gridcells.

The NO_2 VCDs retrieved from both OMI and GOME-2 are much larger than corresponding model results (see Lin et al., 2009). Consequently, top–down emissions derived with the Martin et al. method are 31–160% higher than bottom–up estimates (Table 1), consistent with conclusions in previous studies (Martin et al., 2003, 2006; Jaegle et al., 2005; Wang et al., 2007; Zhang et al., 2007). These top–down estimates are also 4–85% larger than estimates obtained using the Lin et al. method, depending on the choice of satellite retrievals and PBL schemes, consistent with the findings of Lin et al. (2009). While it is possible that bottom–up approaches underestimate Chinese emissions to some extent, the magnitude of the underestimate inferred using the Martin et al. method appears unlikely (Qiang Zhang, Yu Zhao, Yu Lei, personal communication). We speculate that the large emissions estimated based on the Martin et al. method may be due at least in part to errors in the retrieval process contributing most likely to an overestimate of NO_2 VCDs (Folkert Boersma, personal communication; also see Lin et al. (2009) and references therein). Biases in satellite NO_2 VCDs are attributed significantly to systematic errors introduced in the process converting satellite observed radiation to tropospheric NO_2 VCDs (Boersma et al., 2004). These systematic biases lead to consequent uncertainties in top–down emissions estimated with the Martin et al. method, which assumes a linear relation between NO_x emissions and NO_2 retrievals. The Lin et al. method, by comparison, relates NO_x emissions to differences in NO_2 retrievals between satellite instruments observing the atmosphere at different times of day. Furthermore, systematic biases in GOME-2 and OMI NO_2 data are most likely consistent as a result of similar retrieval methods (Lin et al., 2009). Thus impacts of systematic errors in OMI and GOME-2 retrievals may be reduced significantly by the differentiation, leading to closer agreement between top–down and bottom–up emissions. This represents an important advantage of the methodology highlighted by Lin et al. (2009).

Lin et al. (2009) estimated Chinese anthropogenic emissions for July 2008 using the same non-local PBL scheme and satellite retrievals, and suggested a best estimate of emission budget as 5.5 TgN yr^{-1} for East China. The budget is 16% lower than the estimate given here for several reasons. First, Lin et al. (2009) did not allow for a diurnal variation in a priori NO_x emissions, while the best estimate of diurnal profiles for NO_x emissions is included in the present simulation. Lin et al. (2009) found that applying these diurnal profiles in GEOS-Chem led to a 9% increase in top–down emissions. The second factor reflects uncertainties in the estimate of lightning emissions, which are taken in Lin et al. (2009) at the climatological mean of 0.44 TgN yr^{-1} for July derived from the OTD/LIS measurements during 1995–2005 (Lee Murray, personal communication) but are about 84% of the climatology for purposes of this study. Lin et al. (2009) found that 100% higher lightning emissions led to 15% lower anthropogenic emissions in the top–down dataset. Also, the improvement on the Lin et al. method introduced in this study has some impacts on top–down estimates.

6. Concluding remarks

Vertical mixing in the PBL impacts interactions and distributions of air tracers at different altitudes of the lower troposphere (Stull, 2003). Representations of PBL mixing in CTMs influence the simulation of vertical profiles of air tracers, with important consequences for various model studies of tracer sources, sinks and transport. Up to now, the widely used global CTM GEOS-Chem has assumed full mixing in the PBL, which tends to overestimate vertical interactions of tracers in the lower troposphere. To improve the simulation of PBL mixing, the non-local scheme formulated by Holtslag and Boville (1993) was implemented in the CTM as discussed here. This paper analyzes impacts of the non-local scheme for GEOS-Chem simulations of vertical profiles of air tracers, diurnal variations of surface air pollution, and for inverse modeling of NO_x emissions using satellite NO_2 retrievals.

It is found that the non-local scheme significantly improves simulations of the vertical shape of NO_2 and the magnitude of O_3 concentrations in the lower troposphere, as evaluated with aircraft measurements from the NASA INTEX-NA and the NOAA ICARTT campaigns in July–Mid August 2004. In particular, it results in a stronger vertical gradient of NO_2 during the day as compared to simulations using the full mixing assumption, leading to better agreement with aircraft measurements. Additionally, it reduces simulation biases for the lower tropospheric ozone concentrations throughout the day, especially near the surface. Comparisons with the U.S. EPA AQS measurements suggest that the non-local scheme markedly improves simulations of the diurnal variation of surface ozone in July 2004 over the U.S. As compared to the full mixing assumption, the non-local scheme reduces biases by more than 10 ppb for ozone at night and by 2–5 ppb for peak ozone in the afternoon, consistent with the findings of Lin et al. (2008).

The improvement in the simulation of the vertical shape of NO_2 has important implications for applications of GEOS-Chem to the inverse modeling of NO_x emissions using satellite NO_2 retrievals. Top–down estimates of anthropogenic NO_x emissions in East China using the approach proposed by Martin et al. (2003) show, as compared to the non-local scheme, that the full mixing assumption leads to a 3% higher (7% lower) budget for July 2008 when OMI (GOME-2) retrievals from KNMI are used for inverse modeling. Corresponding estimates for January 2009 suggest a 12–14% lower budget when the full mixing assumption is used to drive the simulation. Meanwhile, top–down estimates using the approach proposed by Lin et al. (2009) indicate that the full mixing assumption results in a 12% higher budget in July 2008 and an 8% lower budget in January 2009 as compared with results obtained using the non-local scheme. The top–down estimate combining the non-local scheme and the Lin et al. approach indicates emissions of 6.6 TgN yr^{-1} in July 2008 and 8.0 TgN yr^{-1} in January 2009 for East China, in good agreement with the bottom–up estimates of 5.9 TgN yr^{-1} and 6.8 TgN yr^{-1}, respectively. The seasonality of top–down emissions determined on the basis of the non-local scheme and the Lin et al. approach is also closest to bottom–up estimates, with a January-to-July ratio of ~122% that is similar to the estimates of ~116% by Streets et al. (2003) and Zhang et al. (2009).

Accurate simulation of PBL mixing in global and regional CTMs and climate models poses a difficult challenge, reflecting the chaotic nature of turbulence and the simplification of mixing processes necessary for timely simulations with limited computational resources (Holtslag, 2002; Stull, 2003; Teixeira et al., 2008). Great efforts have been made to improve the understanding of PBL mixing and the performance of PBL schemes (Teixeira et al., 2008), such as the Global Energy and Water Cycle Experiment (GEWEX) Atmospheric Boundary Layer Study (GABLS) (Holtslag, 2006). Various attempts have been implemented to improve the Holtslag and Boville (1993) scheme and other non-local schemes, including parameterizations of PBL depth, non-local momentum mixing, eddy diffusion coefficient, and air entrainment at the PBL top (Vogelezang and Holtslag, 1996; Brown and Grant, 1997; van Meijgaard and van Ulden, 1998; Lock et al., 2000; Noh et al., 2003; Hong et al., 2006; Brown et al., 2008; Sorbjan, 2009). At present, these improvements have not been incorporated into GEOS-Chem due to complications in the implementation (e.g., requirement for additional parameters and longer calculation, etc.); they, however, will be considered in future model development.

Meanwhile, the non-local scheme by Holtslag and Boville (1993) provides an easily implemented approach that has been adopted widely in a range of state-of-the-art CTMs and climate models. As demonstrated here, it results in a more realistic representation of PBL mixing as compared with formulations assuming full mixing. In conclusion, this newly implemented non-local scheme offers an important improvement for a range of GEOS-Chem applications sensitive to the details of PBL mixing, including analysis of data from satellite remote sensing.

Acknowledgments

References

Avery, M.A., Westberg, D.J., Fuelberg, H.E., Newell, R.E., Anderson, B.E., Vay, S.A., Sachse, G.W., Blake, D.R., 2001. Chemical transport across the ITCZ in the central Pacific during an El Nino-Southern Oscillation cold phase event in March–April 1999. Journal of Geophysical Research 106, 32539–32553.

Bertram, T.H., Perring, A.E., Wooldridge, P.J., Crounse, J.D., Kwan, A.J., Wennberg, P.O., Scheuer, E., Dibb, J., Avery, M., Sachse, G., Vay, S.A., Crawford, J.H., McNaughton, C. S., Clarke, A., Pickering, K.E., Fuelberg, H., Huey, G., Blake, D.R., Singh, H.B., Hall, S. R., Shetter, R.E., Fried, A., Heikes, B.G., Cohen, R.C., 2007. Direct measurements of the convective recycling of the upper troposphere. Science 315, 816–820.

Boersma, K.F., Eskes, H.J., Brinksma, E.J., 2004. Error analysis for tropospheric NO_2 retrieval from space. Journal of Geophysical Research 109. doi:10.1029/2003JD003962.

Boersma, K.F., Eskes, H.J., Veefkind, J.P., Brinksma, E.J., van der, A.R.J., Sneep, M., van den Oord, G.H.J., Levelt, P.F., Stammes, P., Gleason, J.F., Bucsela, E.J., 2007. Near-real time retrieval of tropospheric NO_2 from OMI. Atmospheric Chemistry and Physics 7, 2103–2118.

Boersma, K.F., Jacob, D.J., Bucsela, E.J., Perring, A.E., Dirksen, R., Van Der, A.R.J., Yantosca, R.M., Park, R.J., Wenig, M.O., Bertram, T.H., Cohen, R.C., 2008a. Validation of OMI tropospheric NO_2 observations during INTEX-B and application to constrain NO_x emissions over the eastern United States and Mexico. Atmospheric Environment 42, 18. doi:10.1016/j.atmosenv.2008.02.004.

Boersma, K.F., Jacob, D.J., Eskes, H.J., Pinder, R.W., Wang, J., Van Der, A.R.J., 2008b. Intercomparison of SCIAMACHY and OMI tropospheric NO_2 columns: observing the diurnal evolution of chemistry and emissions from space. Journal of Geophysical Research 113, 14. doi:10.1029/2007JD008816.

Brown, A.R., Grant, A.L.M., 1997. Non-local mixing of momentum in the convective boundary layer. Boundary-Layer Meteorology 84, 1–22.

Brown, A.R., Beare, R.J., Edwards, J.M., Lock, A.P., Keogh, S.J., Milton, S.F., Walters, D.N., 2008. Upgrades to the boundary-layer scheme in the met office numerical weather prediction model. Boundary-Layer Meteorology 128, 117–132. doi:10.1007/s10546-008-9275-0.

Collins, W.D., Rasch, P.J., Boville, B.A., Hack, J.J., McCaa, J.R., Williamson, D.L., Briegleb, B.P., Bitz, C.M., Lin, S.J., Zhang, M.H., 2006. The formulation and atmospheric simulation of the Community Atmosphere Model version 3 (CAM3). Journal of Climate 19, 2144–2161.

Emmons, L.K., Pfister, G.G., Edwards, D.P., Gille, J.C., Sachse, G., Blake, D., Wofsy, S., Gerbig, C., Matross, D., Nedelec, P., 2007. Measurements of Pollution in the Troposphere (MOPITT) validation exercises during summer 2004 field campaigns over North America. Journal of Geophysical Research 112. doi:10.1029/2006jd007833.

Emmons, L.K., Edwards, D.P., Deeter, M.N., Gille, J.C., Campos, T., Nedelec, P., Novelli, P., Sachse, G., 2009. Measurements of Pollution in the Troposphere (MOPITT) validation through 2006. Atmospheric Chemistry and Physics 9, 1795–1803.

Fehsenfeld, F.C., Ancellet, G., Bates, T.S., Goldstein, A.H., Hardesty, R.M., Honrath, R., Law, K.S., Lewis, A.C., Leaitch, R., McKeen, S., Meagher, J., Parrish, D.D., Pszenny, A. A.P., Russell, P.B., Schlager, H., Seinfeld, J., Talbot, R., Zbinden, R., 2006. International Consortium for Atmospheric Research on Transport and Transformation (ICARTT): North America to Europe – overview of the 2004 summer field study. Journal of Geophysical Research 111, 36. doi:10.1029/2006jd007829.

Holtslag, A., Boville, B., 1993. Local versus nonlocal boundary-layer diffusion in a global climate model. Journal of Climate 6, 1825.

Holtslag, A.A.M., 2002. Atmospheric boundary layers: modeling and parameterization. In: Encyclopedia of Atmospheric Sciences. Academic Press, pp. 253–261.

Holtslag, B., 2006. Preface – GEWEX Atmospheric Boundary-Layer Study (GABLS) on stable boundary layers. Boundary-Layer Meteorology 118, 243–246. doi:10.1007/s10546-005-9008-6.

Hong, S.Y., Pan, H.L., 1996. Nonlocal boundary layer vertical diffusion in a medium-range forecast model. Monthly Weather Review 124, 2322–2339.

Hong, S.Y., Noh, Y., Dudhia, J., 2006. A new vertical diffusion package with an explicit treatment of entrainment processes. Monthly Weather Review 134, 2318–2341.

Horowitz, L.W., Walters, S., Mauzerall, D.L., Emmons, L.K., Rasch, P.J., Granier, C., Tie, X.X., Lamarque, J.F., Schultz, M.G., Tyndall, G.S., Orlando, J.J., Brasseur, G.P., 2003. A global simulation of tropospheric ozone and related tracers: description and evaluation of MOZART, version 2. Journal of Geophysical Research 108. doi:10.1029/2002jd002853.

Hudman, R.C., Jacob, D.J., Turquety, S., Leibensperger, E.M., Murray, L.T., Wu, S., Gilliland, A.B., Avery, M., Bertram, T.H., Brune, W., Cohen, R.C., Dibb, J.E., Flocke, F.M., Fried, A., Holloway, J., Neuman, J.A., Orville, R., Perring, A., Ren, X., Sachse, G.W., Singh, H.B., Swanson, A., Wooldridge, P.J., 2007. Surface and lightning sources of nitrogen oxides over the United States: magnitudes, chemical evolution, and outflow. Journal of Geophysical Research 112. doi:10.1029/2006jd007912.

Hudman, R.C., Murray, L.T., Jacob, D.J., Millet, D.B., Turquety, S., Wu, S., Blake, D.R., Goldstein, A.H., Holloway, J., Sachse, G.W., 2008. Biogenic versus anthropogenic sources of CO in the United States. Geophysical Research Letters 35. doi:10.1029/2007gl032393.

Jaegle, L., Steinberger, L., Martin, R.V., Chance, K., 2005. Global partitioning of NO_x sources using satellite observations: relative roles of fossil fuel combustion, biomass burning and soil emissions. Faraday Discussion 130. doi:10.1039/b502128f.

Krol, M., Houweling, S., Bregman, B., van den Broek, M., Segers, A., van Velthoven, P., Peters, W., Dentener, F., Bergamaschi, P., 2005. The two-way nested global chemistry-transport zoom model TM5: algorithm and applications. Atmospheric Chemistry and Physics 5, 417–432.

Lin, J.-T., Youn, D., Liang, X.-Z., Wuebbles, D.J., 2008. Global model simulation of summertime U.S. ozone diurnal cycle and its sensitivity to PBL mixing, spatial resolution, and emissions. Atmospheric Environment. doi:10.1016/j.atmosenv.2008.08.012.

Lin, J., McElroy, M.B., Boersma, K.F., 2009. Constraint of anthropogenic NO_x emissions in China from different sectors: a new methodology using multiple satellite retrievals. Atmospheric Chemistry and Physics Discussions.

Lock, A.P., Brown, A.R., Bush, M.R., Martin, G.M., Smith, R.N.B., 2000. A new boundary layer mixing scheme. Part I: scheme description and single-column model tests. Monthly Weather Review 128, 3187–3199.

Louis, J.F., Tiedtke, M., Geleyn, J.F., 1982. A Short History of the PBL Parameterization at ECMWF, ECMWF Workshop on Boundary-Layer Parameterization.

Martin, R.V., Jacob, D.J., Chance, K., Kurosu, T.P., Palmer, P.I., Evans, M.J., 2003. Global inventory of nitrogen oxide emissions constrained by space-based observations of NO_2 columns. Journal of Geophysical Research 108. doi:10.1029/2003JD003453.

Martin, R.V., Sioris, C.E., Chance, K., Ryerson, T.B., Bertram, T.H., Wooldridge, P.J., Cohen, R.C., Andy Neuman, J., Swanson, A., Flocke, F.M., 2006. Evaluation of space-based constraints on global nitrogen oxide emissions with regional aircraft measurements over and downwind of eastern North America. Journal of Geophysical Research 111. doi:10.1029/2005JD006680.

Martin, R.V., 2008. Satellite remote sensing of surface air quality. Atmospheric Environment 42, 7823–7843. doi:10.1016/j.atmosenv.2008.07.018.

McElroy, M.B., Wang, Y.X., 2005. Human and animal wastes: implications for atmospheric N_2O and NO_x. Global Biogeochemical Cycles 19. doi:10.1029/2004GB002429.

Mellor, G.L., Yamada, T., 1982. Development of a turbulence closure-model for geophysical fluid problems. Reviews of Geophysics 20, 851–875.

Mijling, B., Van Der, A.R.J., Boersma, K.F., Roozendael, M.V., DeSmedt, I., Kelder, H.M., 2009. Reductions of NO_2 detected from space during the 2008 Beijing Olympic Games. Geophysical Research Letters 36. doi:10.1029/2009gl038943.

Millet, D.B., Jacob, D.J., Boersma, K.F., Fu, T.M., Kurosu, T.P., Chance, K., Heald, C.L., Guenther, A., 2008. Spatial distribution of isoprene emissions from North America derived from formaldehyde column measurements by the OMI satellite sensor. Journal of Geophysical Research 113. doi:10.1029/2007jd008950.

Noh, Y., Cheon, W.G., Hong, S.Y., Raasch, S., 2003. Improvement of the K-profile model for the planetary boundary layer based on large eddy simulation data. Boundary-Layer Meteorology 107, 401–427.

Olivier, J.G.J., Berdowski, J.J.M., 2001. Global emissions sources and sinks. In: Berdowski, J.J.M., Guicherit, R., Heij, B.J. (Eds.), The Climate System. A.A. Balkema Publishers/Swets & Zeitlinger Publishers, Lisse, The Netherlands.

Pal, J.S., Giorgi, F., Bi, X.Q., Elguindi, N., Solmon, F., Gao, X.J., Rauscher, S.A., Francisco, R., Zakey, A., Winter, J., Ashfaq, M., Syed, F.S., Bell, J.L., Diffenbaugh, N.S., Karmacharya, J., Konare, A., Martinez, D., da Rocha, R.P., Sloan, L.C., Steiner, A.L., 2007. Regional climate modeling for the developing world – the ICTP RegCM3 and RegCNET. Bulletin of the American Meteorological Society 88. doi:10.1175/bams-88-9-1395.

Pickering, K.E., Wang, Y., Tao, W.-K., Price, C., Müller, J.-F., 1998. Vertical distributions of lighting NOx for use in regional and global chemical transport models. Journal of Geophysical Research 103, 14.

Price, C., Penner, J., Prather, M., 1997. NOx from lightning, 1, Global distribution based on lightning physics. Journal of Geophysical Research 102, 12.

Ryerson, T.B., Buhr, M.P., Frost, G.J., Goldan, P.D., Holloway, J.S., Hubler, G., Jobson, B. T., Kuster, W.C., McKeen, S.A., Parrish, D.D., Roberts, J.M., Sueper, D.T., Trainer, M., Williams, J., Fehsenfeld, F.C., 1998. Emissions lifetimes and ozone formation in power plant plumes. Journal of Geophysical Research 103, 22569–22583.

Ryerson, T.B., Huey, L.G., Knapp, K., Neuman, J.A., Parrish, D.D., Sueper, D.T., Fehsenfeld, F.C., 1999. Design and initial characterization of an inlet for gas-phase NO_y measurements from aircraft. Journal of Geophysical Research 104, 5483–5492.

Singh, H.B., Brune, W.H., Crawford, J.H., Jacob, D.J., Russell, P.B., 2006. Overview of the summer 2004 intercontinental chemical transport experiment – North America (INTEX-A). Journal of Geophysical Research 111. doi:10.1029/2006jd007905.

Sorbjan, Z., 2009. Improving non-local parameterization of the convective boundary layer. Boundary-Layer Meteorology 130, 57–69. doi:10.1007/s10546-008-9331-9.

Streets, D.G., Bond, T.C., Carmichael, G.R., Fernandes, S.D., Fu, Q., He, D., Klimont, Z., Nelson, S.M., Tsai, N.Y., Wang, M.Q., Woo, J.-H., Yarber, K.F., 2003. An inventory of gaseous and primary aerosol emissions in Asia in the year 2000. Journal of Geophysical Research 108. doi:10.1029/2002JD003093.

Stull, R.B., 2003. An Introduction to Boundary Layer Meteorology. Kluwer Academic, Boston, p. 670.

Teixeira, J., Stevens, B., Bretherton, C.S., Cederwall, R., Doyle, J.D., Golaz, J.C., Holtslag, A.A.M., Klein, S.A., Lundquist, J.K., Randall, D.A., Siebesma, A.R., Soares, P.M.M., 2008. Parameterization of the atmospheric boundary layer. Bulletin of the American Meteorological Society 89, 453–458. doi:10.1175/bams-89-4-453.

Troen, I., Mahrt, L., 1986. A simple-model of the atmospheric boundary-layer – sensitivity to surface evaporation. Boundary-Layer Meteorology 37, 129–148.

Turquety, S., Logan, J.A., Jacob, D.J., Hudman, R.C., Leung, F.Y., Heald, C.L., Yantosca, R.M., Wu, S.L., Emmons, L.K., Edwards, D.P., Sachse, G.W., 2007. Inventory of boreal fire emissions for North America in 2004: importance of peat burning and pyroconvective injection. Journal of Geophysical Research 112. doi:10.1029/2006jd007281.

van der A, R.J., Eskes, H.J., Boersma, K.F., Noije, T.P.C.v., Roozendael, M.V., DeSmedt, I., Peters, D.H.M.U., Meijer, E.W., 2008. Trends, seasonal variability and dominant NO_x source derived from a ten year record of NO_2 measured from space. Journal of Geophysical Research 113. doi:10.1029/2007JD009021.

van der Werf, G.R., Randerson, J.T., Giglio, L., Collatz, G.J., Kasibhatla, P.S., Arellano, A.F., 2006. Interannual variability in global biomass burning emissions from 1997 to 2004. Atmospheric Chemistry and Physics 6, 3423–3441.

van Meijgaard, E., van Ulden, A.P., 1998. A first order mixing-condensation scheme for nocturnal stratocumulus. Atmospheric Research 45, 253–273.

Vogelezang, D.H.P., Holtslag, A.A.M., 1996. Evaluation and model impacts of alternative boundary-layer height formulations. Boundary-Layer Meteorology 81, 245–269.

Wang, Y., McElroy, M.B., Wang, T., Palmer, P.I., 2004. Asian emissions of CO and NO_x: constraints from aircraft and Chinese station data. Journal of Geophysical Research 109. doi:10.1029/2004JD005250.

Wang, Y., McElroy, M.B., Martin, R.V., Streets, D.G., Zhang, Q., Fu, T.-M., 2007. Seasonal variability of NO_x emissions over east China constrained by satellite observations: implications for combustion and microbial sources. Journal of Geophysical Research 112. doi:10.1029/2006JD007538.

Wesely, M.L., 1989. Parameterization of surface resistances to gaseous dry deposition in regional-scale numerical-models. Atmospheric Environment 23, 1293–1304.

Wesely, M.L., Hicks, B.B., 2000. A review of the current status of knowledge on dry deposition. Atmospheric Environment 34, 2261–2282.

Wild, O., Prather, M.J., 2006. Global tropospheric ozone modeling: quantifying errors due to grid resolution. Journal of Geophysical Research 111. doi:10.1029/2005jd006605.

Yienger, J.J., Levy II, H., 1995. Empirical model of global soil-biogenic NOx emissions. Journal of Geophysical Research 100, 18.

Zhang, L., Jacob, D.J., Bowman, K.W., Logan, J.A., Turquety, S., Hudman, R.C., Li, Q.B., Beer, R., Worden, H.M., Worden, J.R., Rinsland, C.P., Kulawik, S.S., Lampel, M.C., Shephard, M.W., Fisher, B.M., Eldering, A., Avery, M.A., 2006. Ozone–CO correlations determined by the TES satellite instrument in continental outflow regions. Geophysical Research Letters 33. doi:10.1029/2006gl026399.

Zhang, L., Jacob, D.J., Boersma, K.F., Jaffe, D.A., Olson, J.R., Bowman, K.W., Worden, J.R., Thompson, A.M., Avery, M.A., Cohen, R.C., Dibb, J.E., Flocke, F.M., Fuelberg, H.E., Huey, L.G., McMillan, W.W., Singh, H.B., Weinheimer, A.J., 2008. Transpacific transport of ozone pollution and the effect of recent Asian emission increases on air quality in North America: an integrated analysis using satellite, aircraft, ozonesonde, and surface observations. Atmospheric Chemistry and Physics 8, 20.

Zhang, Q., Streets, D.G., He, K., Wang, Y., Richter, A., Burrows, J.P., Uno, I., Jang, C.J., Chen, D., Yao, Z., Lei, Y., 2007. NO_x emission trends for China, 1995–2004: the view from the ground and the view from space. Journal of Geophysical Research 112. doi:10.1029/2007JD008684.

Zhang, Q., Streets, D.G., Carmichael, G.R., He, K., Huo, H., Kannari, A., Klimont, Z., Park, I., Reddy, S., Fu, J.S., Chen, D., Duan, L., Lei, Y., Wang, L., Yao, Z., 2009. Asian emissions in 2006 for the NASA INTEX-B mission. Atmospheric Chemistry and Physics Discussions 9.

Zhao, C., Wang, Y.H., 2009. Assimilated inversion of NO_x emissions over East Asia using OMI NO_2 column measurements. Geophysical Research Letters 36. doi:10.1029/2008gl037123.

Ziemke, J.R., Chandra, S., Duncan, B.N., Froidevaux, L., Bhartia, P.K., Levelt, P.F., Waters, J.W., 2006. Tropospheric ozone determined from aura OMI and MLS: evaluation of measurements and comparison with the Global Modeling initiative's Chemical Transport Model. Journal of Geophysical Research 111. doi:10.1029/2006jd007089.